# An $H_\infty$ Almost Disturbance Decoupling Robust Controller Design for a Piezoelectric Bimorph Actuator with Hysteresis

Ben M. Chen, *Member, IEEE,* Tong H. Lee, *Member, IEEE,*
Chang-Chieh Hang, *Fellow, IEEE*, Yi Guo, and Siri Weerasooriya

*Abstract*— A robust controller design for a piezoelectric bimorph nonlinear actuator is considered in this paper. The nonlinear dynamics of the actuator are first linearized using the stochastic equivalent linearization method and reformulated into a standard almost disturbance decoupling problem. Then a robust controller, which is explicitly parameterized by two tuning parameters, is carried out using a so-called asymptotic time-scale and eigenstructure assignment approach. The parameterized controller can be tuned by adjusting the parameters to achieve disturbance decoupling and other design goals for the problem that we consider. Simulation results of time-domain responses show that the design is very successful in terms of steady-state tracking error and settling time as well as other performances.

*Index Terms*—Actuators, disturbance decoupling, $H_\infty$ control, piezoelectric devices, robust control, suboptimal control.

## I. Introduction to the Problem

**P**IEZOELECTRICITY is a fundamental process in electro-mechanical energy conversion. It relates electric polarization to mechanical stress/strain in piezoelectric materials. Under the direct piezoelectric effect, an electric charge can be observed when the materials are deformed. The converse or the reciprocal piezoelectric effect is when the application of an electric field can cause mechanical stress/strain in the piezo materials. There are numerous piezoelectric materials available today with PZT (lead zirconate titanate), PLZT (lanthanum modified lead zirconate titanate), and PVDF (piezoelectric polymeric polyvinylidene fluoride) to name a few (see [11]).

Piezoelectric structures are widely used in applications that require electrical to mechanical energy conversion coupled with size limitations, precision, and speed of operation. Typical examples are micro-sensors, micro-positioners, speakers, medical diagnostics, shutters and impact print hammers. In most applications, bimorph or stack piezoelectric structures are used because of the relatively high stress/strain to input electric field ratio (see [11]).

The present work is motivated by the possibility of applying piezoelectric micro-actuators in magnetic recording. The exponential growth of area densities seen in magnetic disk
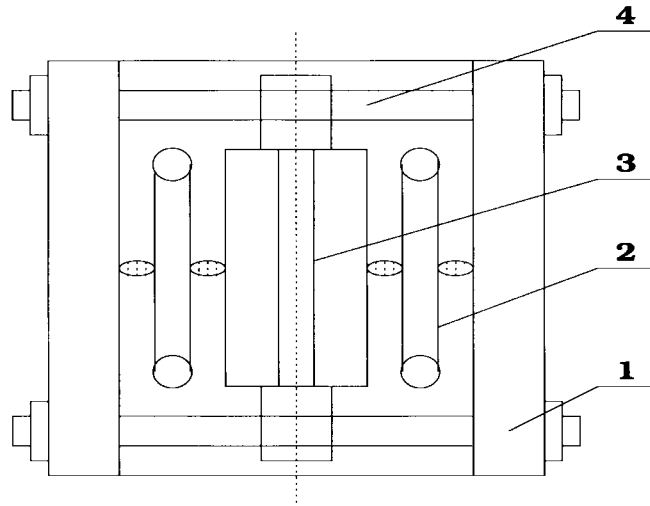
Fig. 1. Structure of a piezoelectric bimorph actuator: 1—base, 2—piezoelectric bimorph beams, 3—moving plate, and 4—guides.

drives means that data tracks and data bits are being placed at closer proximity than ever before. The 25 000 TPI (tracks-per-inch) track densities envisaged at the turn of the century mean that the positioning of the read/write (R/W) heads must be accomplished to within 1 to 2 micro-in error in track following. The closed-loop positioning servo will also be required to have a bandwidth in excess of 1 to 2 kHz to be able to maintain this accuracy at the high spindle speeds required for channel data transfer rates which will be in excess of 200 Mb/s. Such a performance is clearly out of reach with the present voice coil motor (VCM) actuators used in disk drive access systems.

A dual actuator was successfully demonstrated by Tsuchiura *et al.* of Hitachi [18]. In [18], a fine positioner based on a piezoelectric structure was mounted at the end of a primary VCM stage to form the dual actuator. The higher bandwidth of the fine positioner allowed the R/W heads to be accurately positioned. There have been other instances where electromagnetic (see [13]) and electrostatic (see [9]) micro-actuators have been used for fine positioning of R/W heads.

The focus of this paper is to concentrate on the control issues involved in dealing with the nonlinear hysteresis behavior displayed by most piezoelectric actuators. More specifically, we consider a robust controller design for a piezoelectric bimorph actuator as depicted in Fig. 1. A scaled up model
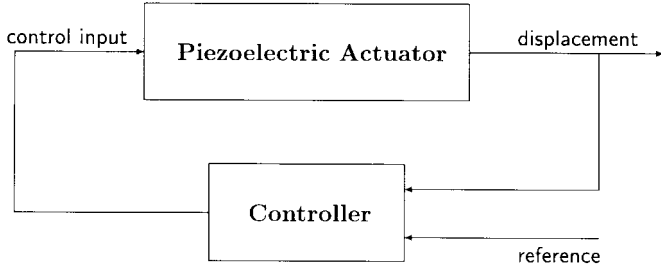
Fig. 2. Piezoelectric bimorph actuator plant with controller.

of this piezoelectric actuator, which is targeted for use in the secondary stage of a future dual actuator for magnetic recording, was actually built and modeled by Low and Guo [11]. It has two pairs of bimorph beams which are subjected to bipolar excitation. The dynamics of the actuator were identified in [11] as a second-order linear model coupled with a hysteresis. The linear model is given by

$$m\ddot{x}_1 + b\dot{x}_1 + kx_1 = k(du - h) \qquad (1)$$

where $m$, $b$, $k$, and $d$ are the tangent mass, damping, stiffness, and effective piezoelectric coefficients, while $u$ is the input voltage that generates excitation forces to the actuator system. The variable $x_1$ is the displacement of the actuator and it is also the only measurement we can have in this system. It should be noted that the working range of the displacement of this actuator is within $\pm 1$ $\mu$m. The variable $h$ is from the hysteretic nonlinear dynamics [11] and is governed by

$$\dot{h} = \alpha d\dot{u} - \beta|\dot{u}|h - \gamma\dot{u}|h| \qquad (2)$$

where $\alpha$, $\beta$, and $\gamma$ are some constants that control the shapes of the hysteresis. For the actuator system that we are considering in this paper, the above coefficients are identified as follows:

$$\left. \begin{array}{rl} m = & 0.01595 \text{ kg} \\ b = & 1.169 \text{ Ns/m} \\ k = & 4385 \text{ N/m} \\ d = & 8.209 \times 10^{-7} \text{ m/V} \\ \alpha = & 0.4297 \\ \beta = & 0.034\,38 \\ \gamma = & -0.002\,865 \end{array} \right\}. \qquad (3)$$

For a more detailed description of this piezoelectric actuator system and the identifications of the above parameters, we refer interested readers to the work of Low and Guo [11]. Our goal of this paper is to design a robust controller as in Fig. 2 that meets the following design specifications.

1) The steady-state tracking errors of the displacement should be less than 1% for any input reference signals that have frequencies ranging from 0 to 30 Hz as the actuator is to be used to track certain color noise type of signals in disk drive systems.

2) The 1% settling time should be as fast as possible (we are able to achieve a 1% settling time less than 0.003 s in our design).

3) The control input signal $u(t)$ should not exceed 112.5 V because of the physical limitation of the piezoelectric materials.

Our approach is as follows: we first use the stochastic equivalent linearization method proposed in Chang [2] to obtain a linearized model for the nonlinear hysteretic dynamics. Then we reformulate our design into a problem of an $H_\infty$ almost disturbance decoupling problem in which the disturbance input is the reference input and the error difference between the hysteretic dynamics and that of its linearized model, while the controlled output is simply the double integration of the tracking error. Thus, our task becomes to design a controller such that when it is applied to the piezoelectric actuator, the overall system is asymptotically stable, and the controlled output, which is corresponding to the tacking error, is as small as possible and decays as fast as possible.

The outline of this paper is as follows: In Section II, a first-order linearized model is obtained for the nonlinear hysteresis using the stochastic equivalent linearization method. Simulation result is also given to show the matching between the nonlinear and linearized models. In Section III, we formulate our controller design into a standard almost disturbance decoupling problem by properly defining the disturbance input and the controlled output. Two integrators are augmented into the original plant to enhance the performance of the overall system. Then a robust controller that is explicitly parameterized by certain tuning parameters and that solves the proposed almost disturbance decoupling problem is carried out using a so-called asymptotic time-scale and eigenstructure assignment technique. In Section IV, we present the final controller and simulation results of our overall control system using MATLAB SIMULINK. We also obtain an explicit relationship between the peak values of the control signal and the tuning parameters of the controller as well as an explicit linear relationship of the maximum trackable frequency, i.e, the corresponding tracking error can be settled to 1%, versus the tuning parameters of the controller. The simulation results of this section clearly show that all the design specifications are met and the overall performance is very satisfactory. Finally, in Section V, we draw our concluding remarks and discuss some implementation issues.

## II. LINEARIZATION OF THE NONLINEAR HYSTERETIC DYNAMICS

We will proceed to linearize the nonlinear hysteretic dynamics of (2) in this section. As pointed out in [2], basically there are three methods available in the literature to linearize the hysteretic type of nonlinear systems. These are 1) the Fokker–Planck equation approach (see, for example, [7]); 2) the perturbation techniques (see, for example, [8] and [12]); and 3) the stochastic linearization approach. All of them have certain advantages and limitations. However, the stochastic linearization technique has the widest range of applications compared to the other methods. This method is based on the concept of replacing the nonlinear system by an "equivalent" linear system in such a way that the "difference" between these two systems is minimized in a certain sense. The technique was initiated by Booton [1]. In this paper, we would just follow the stochastic linearization method given in Chang [2] to obtain a

linear model of the following form:

$$\dot{h} = k_1 \dot{u} + k_2 h \tag{4}$$

for the hysteretic dynamics of (2), where $k_1$ and $k_2$ are the linearization coefficients and are to be determined. The procedure is quite straightforward and proceeds as follows: First we introduce a so-called "difference" function $e$ between $\dot{h}$ of (2) and $\dot{h}$ of (4)

$$e(k_1, k_2) = \alpha d \dot{u} - \beta |\dot{u}| h - \gamma \dot{u} |h| - (k_1 \dot{u} + k_2 h). \tag{5}$$

Then minimizing $\boldsymbol{E}[e^2]$, where $\boldsymbol{E}$ is the expectation operator, with respect to $k_1$ and $k_2$, we obtain

$$\frac{\partial \boldsymbol{E}[e^2]}{\partial k_1} = \frac{\partial \boldsymbol{E}[e^2]}{\partial k_2} = 0 \tag{6}$$

from which the stochastic linearization coefficients $k_1$ and $k_2$ are determined. It turns out that if $h$ and $\dot{u}$ are of zero means and jointly Gaussian, then $k_1$ and $k_2$ can be easily obtained. Let us assume that $h$ and $\dot{u}$ have a joint probability density function

$$f_{\dot{u}h}(\dot{u}, h) = \frac{1}{2\pi\sigma_{\dot{u}}\sigma_h\sqrt{1 - \rho_{\dot{u}h}^2}}$$
$$\cdot \exp\left\{-\frac{\sigma_{\dot{u}}^2 h^2 - 2\sigma_{\dot{u}}\sigma_h\rho_{\dot{u}h}\dot{u}h + \sigma_h^2\dot{u}^2}{2\sigma_{\dot{u}}^2\sigma_h^2(1 - \rho_{\dot{u}h}^2)}\right\} \tag{7}$$

where $\rho_{\dot{u}h}$ is the normalized covariance of $\dot{u}$ and $h$, and $\sigma_{\dot{u}}$ and $\sigma_h$ are the standard deviation of $\dot{u}$ and $h$, respectively. Then the linearization coefficients $k_1$ and $k_2$ can be expressed as the following:

$$k_1 = \alpha d - \beta c_1 - \gamma c_2 \tag{8}$$

and

$$k_2 = -\beta c_3 - \gamma c_4 \tag{9}$$

where $c_1$, $c_2$, $c_3$, and $c_4$ are given by

$$c_1 = 0.7979\sigma_h \cos\left[\tan^{-1}\left(\frac{\sqrt{1 - \rho_{\dot{u}h}^2}}{\rho_{\dot{u}h}}\right)\right] \tag{10}$$

$$c_2 = 0.7979\sigma_h, \quad c_4 = 0.7979\rho_{\dot{u}h}\sigma_{\dot{u}} \tag{11}$$

and

$$c_3 = 0.7979\sigma_{\dot{u}}\left\{1 - \rho_{\dot{u}h}^2\right.$$
$$\left. + \rho_{\dot{u}h}\cos\left[\tan^{-1}\left(\frac{\sqrt{1 - \rho_{\dot{u}h}^2}}{\rho_{\dot{u}h}}\right)\right]\right\}. \tag{12}$$

After many iterations, we found that a sinusoidal excitation $\dot{u}$ with frequencies ranging from 0–100 Hz (the expected working frequency range) and peak magnitude of 50 V, which has a standard deviation of $\sigma_{\dot{u}} = 35$, would yield a suitable linearized model for (2). For this excitation, we obtain $\sigma_h = 5 \times 10^{-7}$, $\rho_{\dot{u}h} = 5 \times 10^{-3}$

$$c_1 = 1.9947 \times 10^{-9}, \quad c_2 = 3.9894 \times 10^{-7} \tag{13}$$

$$c_3 = 27.9260, \quad c_4 = 0.1396 \tag{14}$$

and

$$k_1 = 3.5382 \times 10^{-7}, \quad k_2 = -0.9597. \tag{15}$$

The stochastic linearization model of the nonlinear hysteretic dynamics of (2) is then given by

$$\dot{\hat{h}} = k_1\dot{u} + k_2\hat{h} = 3.5382 \times 10^{-7}\dot{u} - 0.9597\hat{h}. \tag{16}$$

For future use, let us define the linearization error as

$$e_h = h - \hat{h}. \tag{17}$$

Fig. 3 shows the open-loop simulation results of the nonlinear hysteresis and its linearized model, as well as their error for a sine wave input signal $u$ with a peak value of 5 V. The results are quite satisfactory. Here we should note that because of the nature of our approach in controller design later in the next section, the variation of the linearized model within certain range, which might result in larger linearization error, $e_h$, will not affect much the overall performance of the closed-loop system. We will formulate $e_h$ as a disturbance input and our controller will automatically reject it from the output response.

## III. AN $H_\infty$ ALMOST DISTURBANCE DECOUPLING PROBLEM AND ITS SOLUTION

This section is the heart of this paper. We will first formulate our control system design for the piezoelectric bimorph actuator into a standard $H_\infty$ almost disturbance decoupling problem, and then apply the results of Chen et al. [5] to check the solvability of the proposed problem. Finally, we will utilize the results of Ozcetin et al. [14] as well as Chen et al. [6] to find an internally stabilizing controller that solves the proposed almost disturbance decoupling problem. Of course, most importantly, the resulting closed-loop system and its responses should meet all the design specifications as listed in Section I. To do this, we will have to convert the dynamic model of (1) with the linearized model of the hysteresis into a state-space form. Let us first define a new state variable

$$v = \hat{h} - k_1 u. \tag{18}$$

Then from (16), we have

$$\dot{v} = \dot{\hat{h}} - k_1\dot{u} = k_2\hat{h} = k_2 v + k_1 k_2 u. \tag{19}$$

Substituting (17) and (18) into (1), we obtain

$$\ddot{x}_1 + \frac{b}{m}\dot{x}_1 + \frac{k}{m}x_1 + \frac{k}{m}v = \frac{k(d - k_1)}{m}u - \frac{k}{m}e_h. \tag{20}$$

The overall controller structure of our approach is then depicted Fig. 4. Note that in Fig. 4 we have augmented two integrators after $e$, the tracking error between the displacement $x_1$ and the reference input signal $r$. We have observed a very interesting property of this problem, i.e., the more integrators that we augment after the tracking error $e$, the smaller tracking error we can achieve for the same level of control input $u$. Because our control input $u$ is limited to the range from $-112.5$ to $112.5$ V, it turns out that two integrators are needed in order to meet all the design specifications. It is clear to see that the augmented system has an order of five. Next, let us define the state of the augmented system as

$$x = (x_1 \quad \dot{x}_1 \quad v \quad x_4 \quad x_5)' \tag{21}$$

and the measurement output

$$y = \begin{pmatrix} y_1 \\ y_2 \\ y_3 \end{pmatrix} = \begin{pmatrix} x_1 \\ x_4 \\ x_5 \end{pmatrix} \tag{22}$$

$h$ (solid), $\hat{h}$ (dashed), and $e_h$ (dash-dotted)
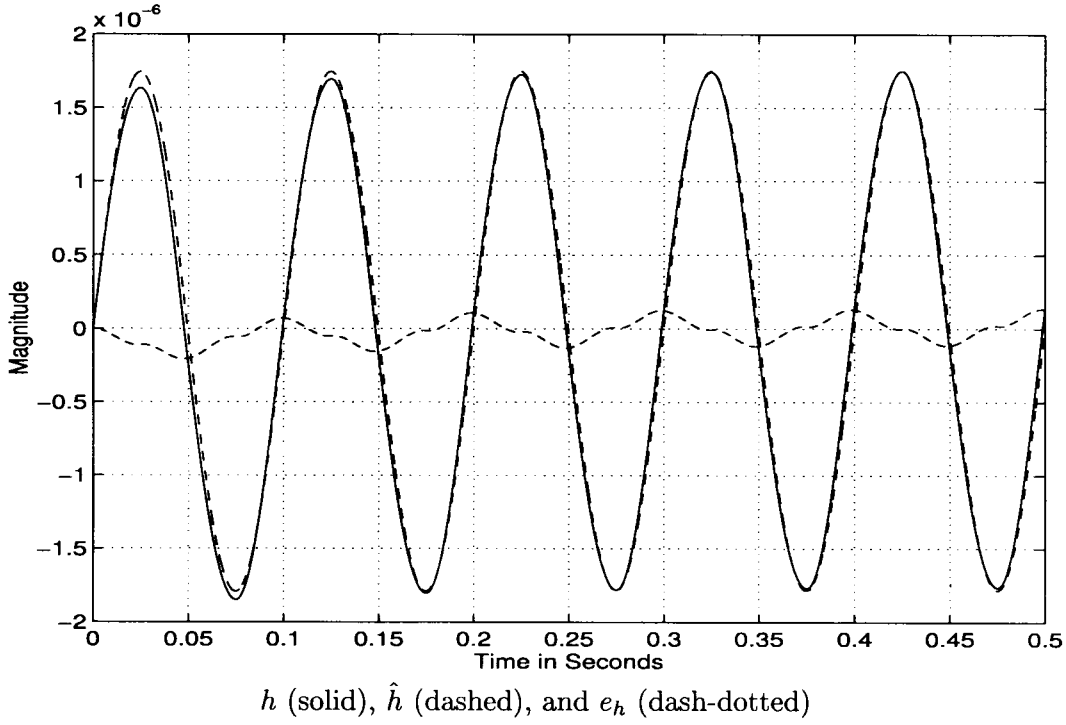
Fig. 3. Responses of the hysteresis and its linearized model to a sine input signal: $h$ (solid), $\hat{h}$ (dashed), and $e_h$ (dash-dotted).

i.e., the original measurement of displacement $x_1$ plus two augmented states. The auxiliary disturbance input is

$$w = \begin{pmatrix} e_h \\ r \end{pmatrix} \tag{23}$$

and the output to be controlled, $z$, is simply the double integration of the tracking error. The state-space model of the overall augmented system is then given by

$$\Sigma: \begin{cases} \dot{x} = Ax + Bu + Ew \\ y = C_1 x + D_1 w \\ z = C_2 x + D_2 u \end{cases} \tag{24}$$

with

$$A = \begin{bmatrix} 0 & 1 & 0 & 0 & 0 \\ -k/m & -b/m & -k/m & 0 & 0 \\ 0 & 0 & k_2 & 0 & 0 \\ 1 & 0 & 0 & 0 & 0 \\ 0 & 0 & 0 & 1 & 0 \end{bmatrix}$$

$$= \begin{bmatrix} 0 & 1 & 0 & 0 & 0 \\ -274\,921.63 & -73.2915 & -274\,921.63 & 0 & 0 \\ 0 & 0 & -0.9597 & 0 & 0 \\ 1 & 0 & 0 & 0 & 0 \\ 0 & 0 & 0 & 1 & 0 \end{bmatrix} \tag{25}$$

$$B = \begin{bmatrix} 0 \\ k(d - k_1)/m \\ k_1 k_2 \\ 0 \\ 0 \end{bmatrix} = \begin{bmatrix} 0 \\ 0.1284 \\ -3.3956 \times 10^{-7} \\ 0 \\ 0 \end{bmatrix} \tag{26}$$

$$E = \begin{bmatrix} 0 & 0 \\ -k/m & 0 \\ 0 & 0 \\ 0 & -1 \\ 0 & 0 \end{bmatrix} = \begin{bmatrix} 0 & 0 \\ -274\,921.63 & 0 \\ 0 & 0 \\ 0 & -1 \\ 0 & 0 \end{bmatrix} \tag{27}$$

and

$$C_1 = \begin{bmatrix} 1 & 0 & 0 & 0 & 0 \\ 0 & 0 & 0 & 1 & 0 \\ 0 & 0 & 0 & 0 & 1 \end{bmatrix}, \quad D_1 = \begin{bmatrix} 0 & 0 \\ 0 & 0 \\ 0 & 0 \end{bmatrix},$$

$$C_2 = \begin{bmatrix} 0 & 0 & 0 & 0 & 1 \end{bmatrix}, \quad D_2 = 0. \tag{28}$$

The $H_\infty$ almost disturbance decoupling problem is to design a parameterized proper controller of the form

$$\Sigma_c(\varepsilon_1, \varepsilon_2): \begin{cases} \dot{x}_c = A_c(\varepsilon_1, \varepsilon_2)x_c + B_c(\varepsilon_1, \varepsilon_2)y \\ u = C_c(\varepsilon_1, \varepsilon_2)x_c + D_c(\varepsilon_1, \varepsilon_2)y \end{cases} \tag{29}$$

which has the following properties.

1) *Internal Stability:* There exist scalars $\varepsilon_1^* > 0$ and $\varepsilon_2^* > 0$ such that for all $0 < \varepsilon_1 < \varepsilon_1^*$ and $0 < \varepsilon_2 < \varepsilon_2^*$, the closed-loop system comprising $\Sigma$ and the controller $\Sigma_c(\varepsilon_1, \varepsilon_2)$ is asymptotically stable. That is for all $0 < \varepsilon_1 < \varepsilon_1^*$ and $0 < \varepsilon_2 < \varepsilon_2^*$, the following matrix:

$$A_{cl}(\varepsilon_1, \varepsilon_2) = \begin{bmatrix} A + BD_c(\varepsilon_1, \varepsilon_2)C_1 & BC_c(\varepsilon_1, \varepsilon_2) \\ B_c(\varepsilon_1, \varepsilon_2)C_1 & A_c(\varepsilon_1, \varepsilon_2) \end{bmatrix} \tag{30}$$

has all its eigenvalues in the open left-half complex plane.
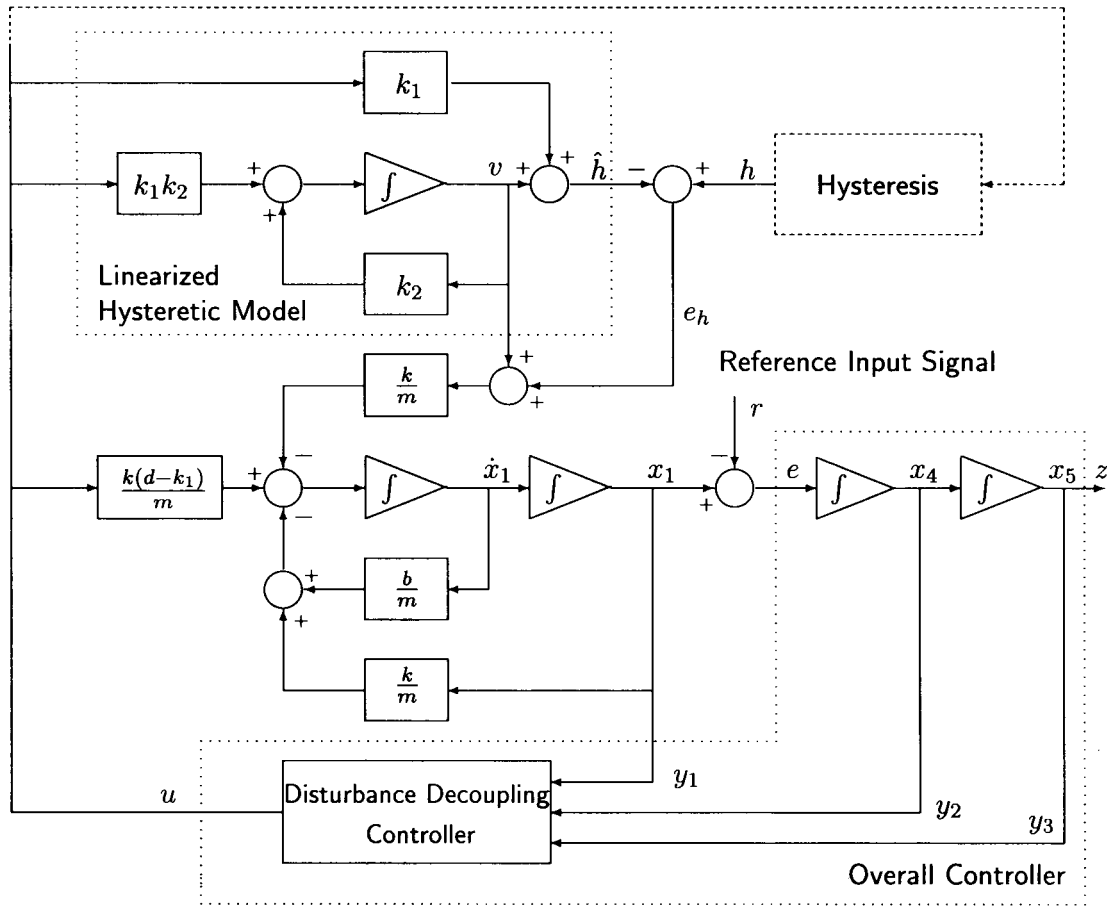
Fig. 4. Augmented linearized model with disturbance decoupling controller.

2) *Disturbance Rejection:* The $H_\infty$-norm of the closed-loop transfer function matrix from the disturbance input $w$ to the output to be controlled $z$, say $T_{zw}(\varepsilon_1, \varepsilon_2, s)$, satisfying

$$\|T_{zw}(\varepsilon_1, \varepsilon_2, s)\|_\infty \to 0 \quad \text{as} \quad \varepsilon_1 \to 0 \quad \text{and} \quad \varepsilon_2 \to 0 \tag{31}$$

where the $H_\infty$-norm of $T_{zw}(\varepsilon_1, \varepsilon_2, s)$ is defined as usual as

$$\|T_{zw}(\varepsilon_1, \varepsilon_2, s)\|_\infty := \sup_{\omega \in [0, \infty)} \sigma_{\max}[T_{zw}(\varepsilon_1, \varepsilon_2, j\omega)] \tag{32}$$

and where $\sigma_{\max}[\cdot]$ denotes the largest singular value.

We also say that the controller $\Sigma_c(\varepsilon_1, \varepsilon_2)$ of (29) solves the almost disturbance decoupling problem for $\Sigma$ of (24) if the above two conditions are satisfied. The problem of almost disturbance decoupling was first introduced by Willems (see [19] for a recent result and related references). It has many applications. Recently, Stoorvogel [17] had obtained a very interesting interconnection between the $H_\infty$ optimal control problem and the disturbance decoupling problem. The necessary and sufficient conditions under which the almost disturbance decoupling problem for $\Sigma$ is solvable, i.e., there

exists a parameterized controller that satisfies the above mentioned two properties, can be found in [19] for strictly proper systems and in [5] for general nonstrictly proper systems. The solution for the general almost disturbance decoupling problem, if existent, can be found in Ozcetin *et al.* [14]. In fact, one can also obtain such a controller using the technique of the so-called closed-loop transfer recovery design proposed in Chen *et al.* [6]. We will discuss this issue further later when it comes to designing the controller.

For the problem that we are considering here, it is simple to verify using the Linear Systems Toolbox [10] that the system $\Sigma$ of (24) has the following properties.

1) The subsystem $(A, B, C_2, D_2)$ is invertible and of minimum phase with one invariant zero at $-1.6867$. It also has one infinite zero of order 4.
2) The subsystem $(A, E, C_1, D_1)$ is left invertible and of minimum phase with one invariant zero at $-0.9597$ and two infinite zeros of orders 1 and 2, respectively.

Then it follows from [19] or [5] that the $H_\infty$ almost disturbance decoupling problem for this $\Sigma$ is solvable. In fact, following the results of Ozcetin *et al.* [14] or Chen *et al.* [6], one can design either a full-order observer-based controller or a reduced order observer-based controller to solve this problem. For the full-order observer-based controller, the order
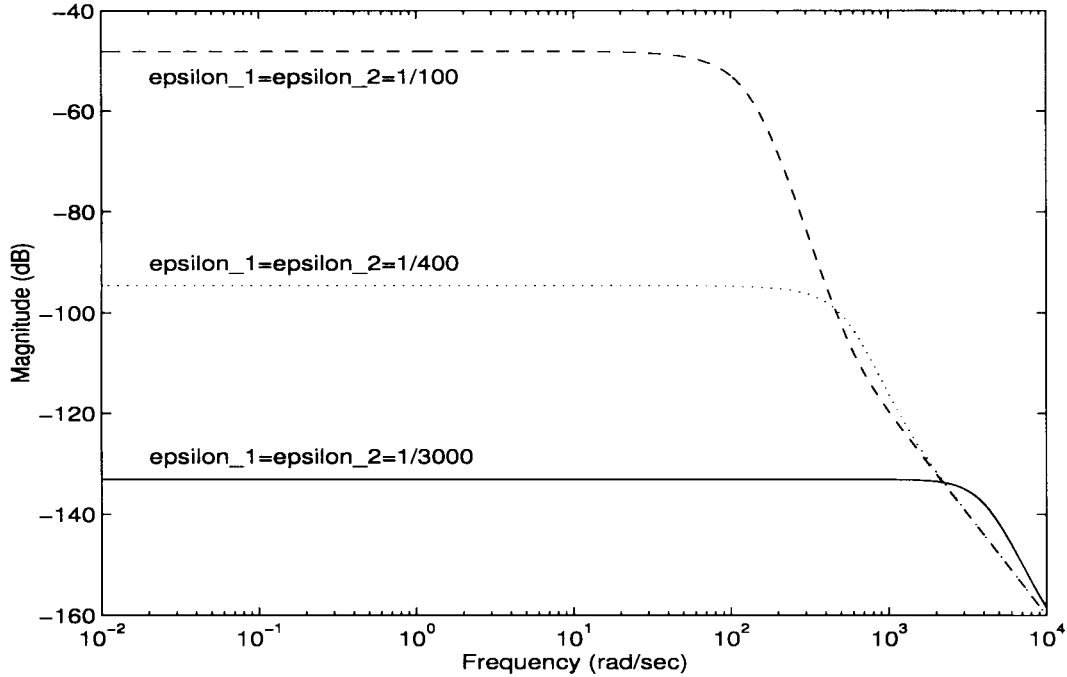
Fig. 5. Maximum singular values of the closed-loop transfer function $T_{zw}(\varepsilon_1, \varepsilon_2, s)$.

of the disturbance decoupling controller (see Fig. 4) will be 5 and the order of the final overall controller (again see Fig. 4) will be 7 (the disturbance decoupling controller plus two integrators). On the other hand, if we use a reduced order observer in the disturbance decoupling controller, the total order of the resulting final overall controller will be reduced to 4. From the practical point of view, the latter is much more desirable than the former. Thus, in what follows we will only focus on the controller design based on a reduced order observer. For the disturbance decoupling problem, we can separate our controller design into two steps.

1) In the first step, we assume that all five states of $\Sigma$ in (24) are available and then design a static and parameterized state feedback control law

$$u = F(\varepsilon_1)x \qquad (33)$$

such that it solves the almost disturbance decoupling problem for the state feedback case, i.e., $y = x$, by adjusting the tuning parameter $\varepsilon_1$ to an appropriate value.

2) In the second step, we follow the procedure of Chen *et al.* [6] to design a reduced order observer-based controller. It has a parameterized reduced order observer gain matrix $K_2(\varepsilon_2)$ that can be tuned to recover the performance achieved by the state feedback control law in the first step.

We will use the asymptotic time-scale and eigenstructure assignment (ATEA) design method proposed in Ozcetin *et al.* [14] and Chen *et al.* [6] to construct both the state feedback law and the reduced order observer gain. The ATEA design method is decentralized in nature. It was initiated by Saberi and Sannuti [15] while the detailed proof of the algorithm,

especially the multi time-scale case, was completed in Chen [3]. It uses the special coordinate basis [16] of the given system. The specified finite eigenstructure of the closed-loop system is assigned appropriately by working with subsystems which represent the finite zero structure of the given system. Similarly, the specified asymptotically infinite eigenstructure of the closed-loop system is assigned appropriately by working with the subsystems which represent the infinite zero structure of the given system. Unfortunately, because of the complexity of the algorithm and the background materials involved in it, it is impossible to present the detailed procedure of the ATEA method here in this paper. We refer the interested readers to Ozcetin *et al.* [14] and Chen *et al.* [6] for details. We would like to note that in principle, one can also apply the ARE (algebraic Riccati equation) based $H_\infty$ optimization technique (see for example Zhou and Khargonekar [20]) to solve this problem. However, because the numerical conditions of our system, $\Sigma$, are very bad, we are unable to obtain any satisfactory solution from the ARE approach. We cannot get any meaningful solution for the associated $H_\infty$-ARE in MATLAB. In this sense and at least for this problem, the ATEA method is much more powerful than the ARE one. The software realization of the ATEA algorithm can be found in the Linear Systems and Control Toolbox developed by Chen [4]. The following is a closed-form solution of the static state feedback parameterized gain matrix $F(\varepsilon_1)$ obtained using the ATEA method in (34), shown at the bottom of the next page, where $\varepsilon_1$ is the tuning parameter that can be adjusted to achieve almost disturbance decoupling. It can be verified that the closed-loop system matrix, $A + BF(\varepsilon_1)$ is asymptotically stable for all $0 < \varepsilon_1 < \infty$ and the closed-loop transfer function from the disturbance $w$ to the controlled output $z$, $T_{zw}(\varepsilon_1, s)$,
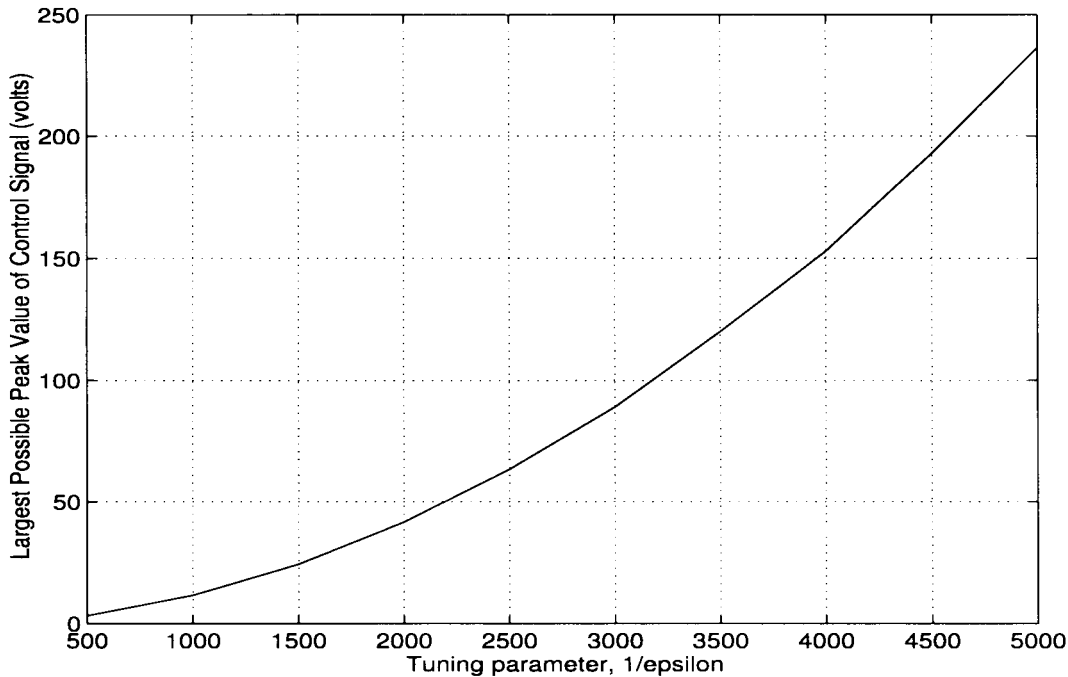
Fig. 6. Parameter $1/\varepsilon$ versus the maximum peak of $u$ in worst initial error situations.

satisfying

$$
\begin{aligned}
\|T_{zw}(\varepsilon_1, s)\|_\infty &= \|[C_2 + D_2 F(\varepsilon_1)] \\
&\quad \cdot [sI - A - BF(\varepsilon_1)]^{-1} E\|_\infty \to 0 \\
&\quad \text{as} \quad \varepsilon_1 \to 0.
\end{aligned}
\tag{35}
$$

The next step is to design a reduced order observer-based controller that will recover the performance of the above state feedback control law. First, let us perform the following nonsingular (permutation) state transformation to the system $\Sigma$ of (24):

$$
x = T\tilde{x}
\tag{36}
$$

where

$$
T = \begin{bmatrix} 1 & 0 & 0 & 0 & 0 \\ 0 & 0 & 0 & 1 & 0 \\ 0 & 0 & 0 & 0 & 1 \\ 0 & 1 & 0 & 0 & 0 \\ 0 & 0 & 1 & 0 & 0 \end{bmatrix}
\tag{37}
$$

such that the transformed measurement matrix has the form of

$$
C_1 T = \begin{bmatrix} 1 & 0 & 0 & 0 & 0 \\ 0 & 1 & 0 & 0 & 0 \\ 0 & 0 & 1 & 0 & 0 \end{bmatrix} = [I_3 \quad 0].
\tag{38}
$$

Clearly, the first three states of the transformed system, or $x_1$, $x_4$, and $x_5$ of the original system $\Sigma$ in (24), need not be estimated as they are already available from the measurement

output. Let us now partition the transformed system as follows:

$$
\begin{aligned}
T^{-1}AT &= \begin{bmatrix} A_{11} & A_{12} \\ \hline A_{21} & A_{22} \end{bmatrix} \\
&= \begin{bmatrix} 0 & 0 & 0 & 1 & 0 \\ 1 & 0 & 0 & 0 & 0 \\ 0 & 1 & 0 & 0 & 0 \\ \hline -274\,921.63 & 0 & 0 & -73.2915 & -274\,921.63 \\ 0 & 0 & 0 & 0 & -0.9597 \end{bmatrix}
\end{aligned}
\tag{39}
$$

$$
T^{-1}B = \begin{bmatrix} B_1 \\ \hline B_2 \end{bmatrix} = \begin{bmatrix} 0 \\ 0 \\ 0 \\ \hline 0.128\,41 \\ -3.395\,61 \times 10^{-7} \end{bmatrix}
$$

$$
T^{-1}E = \begin{bmatrix} E_1 \\ \hline E_2 \end{bmatrix} = \begin{bmatrix} 0 & 0 \\ 0 & -1 \\ 0 & 0 \\ \hline -274\,921.63 & 0 \\ 0 & 0 \end{bmatrix}.
\tag{40}
$$

Also, we partition (41) and (42), shown at the bottom of the next page. Then the reduced-order observer-based controller (see Chen *et al.* [6]) is given as in the form of (29) with

$$
\begin{aligned}
A_c(\varepsilon_1, \varepsilon_2) &= A_{22} + K_2(\varepsilon_2)A_{12} + B_2 F_2(\varepsilon_1) \\
&\quad + K_2(\varepsilon_2)B_1 F_2(\varepsilon_1)
\end{aligned}
\tag{43}
$$

$$
F(\varepsilon_1) = [(2.141 \times 10^6 - 62.3/\varepsilon_1^2) \quad (570.7619 - 31.15/\varepsilon_1) \quad 2.141 \times 10^6 \quad -62.3/\varepsilon_1^3 \quad -31.15/\varepsilon_1^4]
\tag{34}
$$

$$B_c(\varepsilon_1, \varepsilon_2) = A_{21} + K_2(\varepsilon_2)A_{11} - [A_{22} + K_2(\varepsilon_2)A_{12}]K_2(\varepsilon_2)$$
$$+ [B_2 + K_2(\varepsilon_2)B_1][F_1(\varepsilon_1) - F_2(\varepsilon_1)K_2(\varepsilon_2)] \tag{44}$$

$$C_c(\varepsilon_1, \varepsilon_2) = F_2(\varepsilon_1) \tag{45}$$

$$D_c(\varepsilon_1, \varepsilon_2) = F_1(\varepsilon_1) - F_2(\varepsilon_1)K_2(\varepsilon_2) \tag{46}$$

where $K_2(\varepsilon_2)$ is the parameterized reduced order observer gain matrix and is to be designed such that $A_{22} + K_2(\varepsilon_2)A_{12}$ is asymptotically stable for sufficiently small $\varepsilon_2$ and also

$$\|[sI - A_{22} - K_2(\varepsilon_2)A_{12}]^{-1}[E_2 + K_2(\varepsilon_2)E_1]\|_\infty \to 0$$
$$\text{as} \quad \varepsilon_2 \to 0. \tag{47}$$

Again, using the procedure of Chen *et al.* [6] and the software package of Chen [4], we obtained the following parameterized reduced order observer gain matrix:

$$K_2(\varepsilon_2) = \begin{bmatrix} 73.2915 - 1/\varepsilon_2 & 0 & 0 \\ 0 & 0 & 0 \end{bmatrix}. \tag{48}$$

Then the explicitly parameterized matrices of the state-space model of the reduced order observer-based controller are given by that shown in (49)–(54), shown at the bottom of the page.

The overall closed-loop system comprising the system $\Sigma$ of (24) and the above controller would be asymptotically stable as long as $\varepsilon_1 \in (0, \infty)$ and $\varepsilon_2 \in (0, \infty)$. In fact, the closed-loop poles are exactly located at $-1.6867$, two pairs at $-1/\varepsilon_1 \pm j1/\varepsilon_1$, $-0.9597$ and $-1/\varepsilon_2$. The plots of the maximum singular values of the closed-loop transfer function matrix from the disturbance $w$ to the controlled output $z$, namely $T_{zw}(\varepsilon_1, \varepsilon_2, s)$, for several pairs of $\varepsilon_1$ and $\varepsilon_2$, i.e.,

$\varepsilon_1 = \varepsilon_2 = 1/100$, $\varepsilon_1 = \varepsilon_2 = 1/400$, and $\varepsilon_1 = \varepsilon_2 = 1/3000$, in Fig. 5 show that as $\varepsilon_1$ and $\varepsilon_2$ become smaller and smaller, the $H_\infty$ norms of $T_{zw}(\varepsilon_1, \varepsilon_2, s)$ are also smaller and smaller. Hence, almost disturbance decoupling is indeed achieved. These are the properties of our control system in the frequency domain. We will address in the next section its time domain properties, which of course are much more important as all the design specifications are in the time domain.

## IV. FINAL CONTROLLER AND SIMULATION RESULTS OF THE OVERALL CONTROL SYSTEMS

In this section, we will put our design in the previous section into a final controller as depicted in Fig. 2. It is simple to derive the state-space model of the final overall controller by observing its interconnection with the disturbance decoupling controller $\Sigma_c(\varepsilon_1, \varepsilon_2)$ of (29) (see Fig. 3). We will also present simulation results of the responses of the overall design to several different types of reference input signals. They clearly show that all the design specifications are successfully achieved. Furthermore, because our controller is explicitly parameterized by two tuning parameters, it is very easy to be adjusted to meet other design specifications without going through all over again from the beginning. This will also be discussed in the following.

As mentioned earlier, the final overall controller of our design will be order of four, of which two are from the disturbance decoupling controller and two from the augmented integrators. It has two inputs: one is the displacement $x_1$ and the other is the reference signal $r$. It is straightforward to

$$F(\varepsilon_1)T = [F_1(\varepsilon_1) \mid F_2(\varepsilon_1)] \tag{41}$$
$$= [(2.141 \times 10^6 - 62.3/\varepsilon_1^2) \quad -62.3/\varepsilon_1^3 \quad -31.15/\varepsilon_1^4 \mid (570.7619 - 31.15/\varepsilon_1) \quad 2.141 \times 10^6] \tag{42}$$

$$A_c(\varepsilon_1, \varepsilon_2) = \begin{bmatrix} 73.2915 - 4/\varepsilon_1 - 1/\varepsilon_2 & 0 \\ -1.9381 \times 10^{-4} + 1.0577 \times 10^{-5}/\varepsilon_1 & -1.6867 \end{bmatrix} \tag{49}$$

$$C_c(\varepsilon_1, \varepsilon_2) = [570.7619 - 31.15/\varepsilon_1 \quad 2140967] \tag{50}$$

$$D_c(\varepsilon_1, \varepsilon_2) = \begin{bmatrix} 2099135.4 - 62.3/\varepsilon_1^2 + 2283.0476/\varepsilon_1 + 570.7619/\varepsilon_2 - 31.15/(\varepsilon_1\varepsilon_2) \\ -62.3/\varepsilon_1^3 \\ -31.15/\varepsilon_1^4 \end{bmatrix}' \tag{51}$$

and

$$B_c(\varepsilon_1, \varepsilon_2) = \begin{bmatrix} \psi_1 & -8/\varepsilon_1^3 & -4/\varepsilon_1^4 \\ \psi_2 & 2.1155 \times 10^{-5}/\varepsilon_1^3 & 1.0577 \times 10^{-5}/\varepsilon_1^4 \end{bmatrix} \tag{52}$$

where

$$\psi_1 = -5731.6533 - 8/\varepsilon_1^2 + 293.1661/\varepsilon_1 - 1/\varepsilon_2^2 + 146.5831/\varepsilon_2 - 4/(\varepsilon_1\varepsilon_2) \tag{53}$$

and

$$\psi_2 = -0.7128 + 2.1155 \times 10^{-5}/\varepsilon_1^2 - 7.7523 \times 10^{-4}/\varepsilon_1 - 1.9381 \times 10^{-4}/\varepsilon_2 + 1.0577 \times 10^{-5}/(\varepsilon_1\varepsilon_2) \tag{54}$$
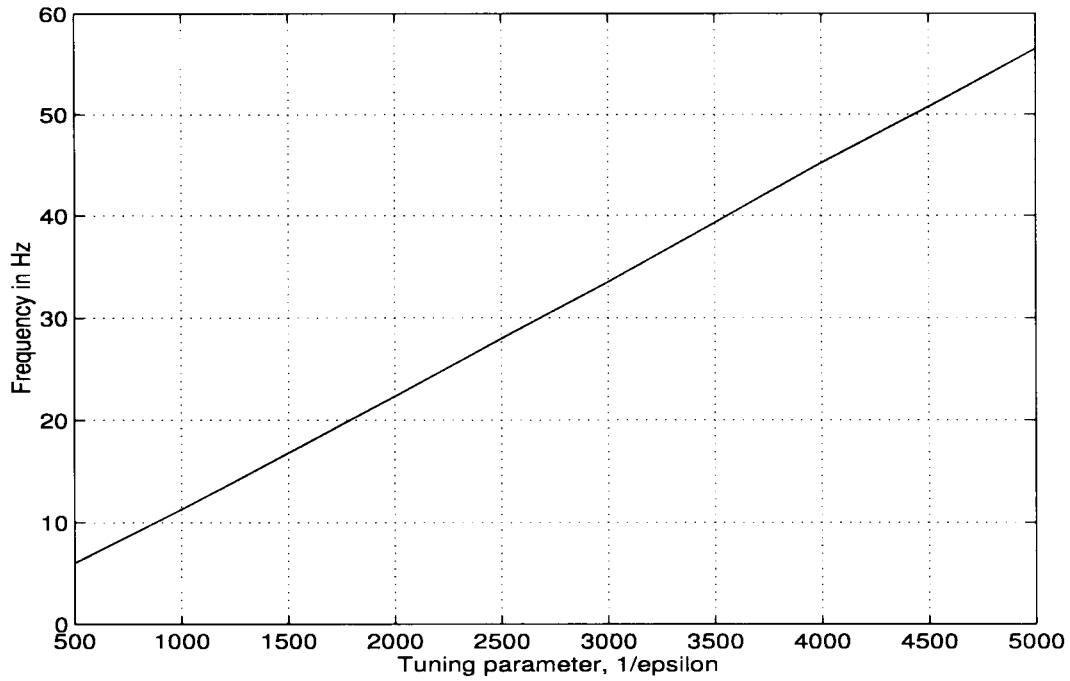
Fig. 7. Parameter $1/\varepsilon$ versus the maximum frequency of $r$ that has 1% tracking error.
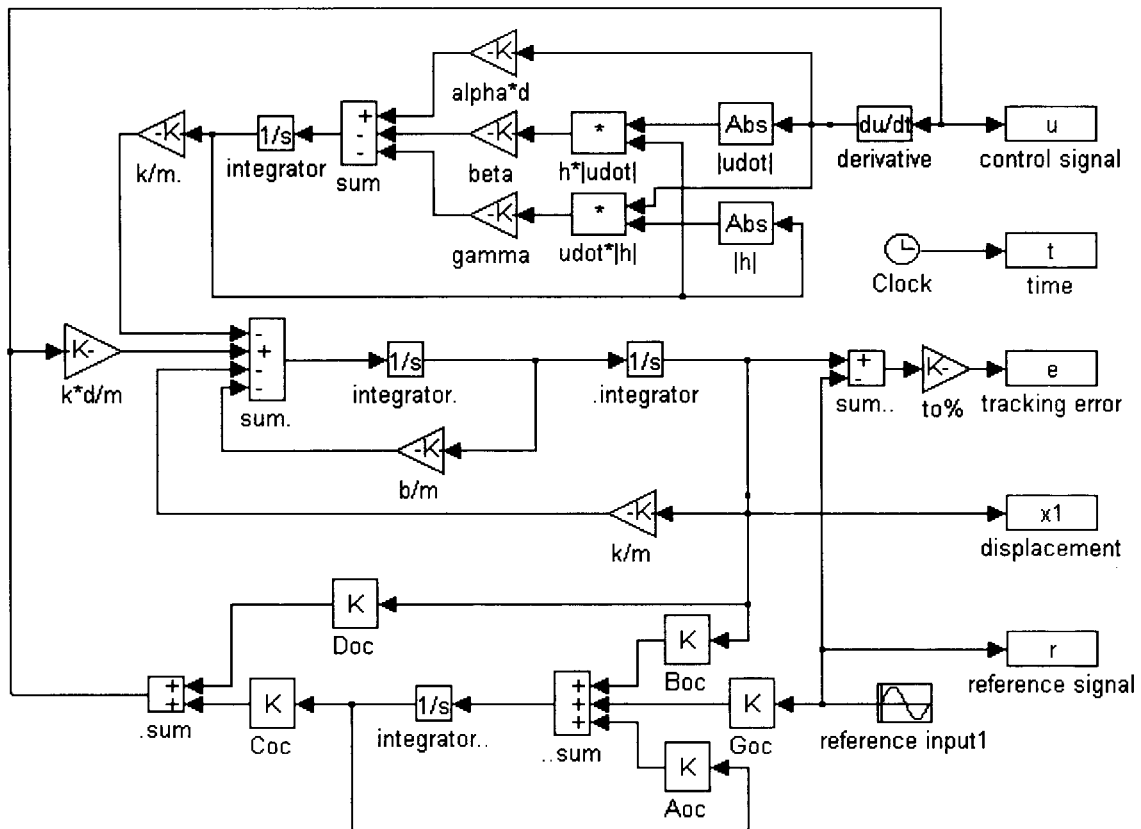


Fig. 8. Simulation block diagram for the overall piezoelectric actuator control system.
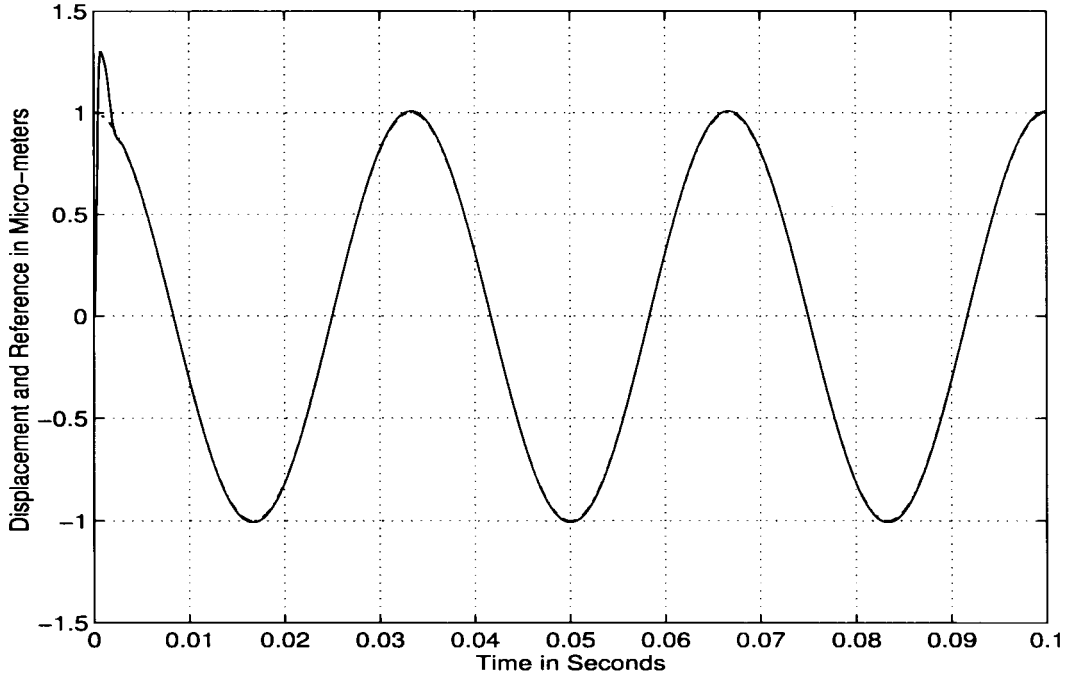
Fig. 9. Responses of the displacement and the 30-Hz cosine reference signal.

verify that the state-space model of the final overall controller is given by (55)–(59), shown at the bottom of the page. There are some very interesting and very useful properties of the above parameterized controller. After repeatedly simulating the overall design, we found that the maximum peak values of the control signal $u$ is independent of the frequencies of the reference signals. It is only dependent on the initial error between displacement, $x_1$, and the reference, $r$. The larger the initial error is, the bigger peak occurs in $u$. Because the working range of our actuator is within $\pm 1$ $\mu$m. We will assume that the largest magnitude of the initial error in any situation should not be larger that 1 $\mu$m. This assumption is

zero before the system is to track any reference and hence the magnitude of initial tracking error can never be larger than 1 $\mu$m. Let us consider the worst case, i.e., the magnitude of the initial error is 1 $\mu$m and also for simplicity of presentation, we now set the two tuning parameters to be equal, i.e., $\varepsilon_1 = \varepsilon_2 = \varepsilon$. Then interestingly, we are able to obtain a clear relationship between the tuning parameter $1/\varepsilon$ and the maximum peak of $u$. The result is plotted in Fig. 6. We also found that the tracking error is independent of initial errors. It only depends on the frequencies of the references, i.e., the larger frequency the reference signal $r$ has, the larger tracking error occurs. Again, we can obtain a simple and

$$\Sigma_{oc}(\varepsilon_1, \varepsilon_2): \quad \begin{cases} \dot{x}_{oc} = A_{oc}(\varepsilon_1, \varepsilon_2)x_{oc} + B_{oc}(\varepsilon_1, \varepsilon_2)x_1 + G_{oc}r \\ u = C_{oc}(\varepsilon_1, \varepsilon_2)x_{oc} + D_{oc}(\varepsilon_1, \varepsilon_2)x_1 \end{cases} \tag{55}$$

$$A_{oc} = \begin{bmatrix} 73.2915 - 4/\varepsilon_1 - 1/\varepsilon_2 & 0 & -8/\varepsilon_1^3 & -4/\varepsilon_1^4 \\ -1.9381 \times 10^{-4} + 1.0577 \times 10^{-5}/\varepsilon_1 & -1.6867 & 2.1155 \times 10^{-5}/\varepsilon_1^3 & 1.0577 \times 10^{-5}/\varepsilon_1^4 \\ 0 & 0 & 0 & 0 \\ 0 & 0 & 1 & 0 \end{bmatrix} \tag{56}$$

$$G_{oc} = \begin{bmatrix} 0 \\ 0 \\ -1 \\ 0 \end{bmatrix}, \quad B_{oc}(\varepsilon_1, \varepsilon_2) = \begin{bmatrix} \psi_1 \\ \psi_2 \\ 1 \\ 0 \end{bmatrix} \tag{57}$$

$$C_{oc}(\varepsilon_1, \varepsilon_2) = [570.7619 - 31.15/\varepsilon_1 \quad 2140967 \quad -62.3/\varepsilon_1^3 \quad -31.15/\varepsilon_1^4] \tag{58}$$

and

$$D_{oc}(\varepsilon_1, \varepsilon_2) = 2099135.4 - 62.3/\varepsilon_1^2 + 2283.0476/\varepsilon_1 + 570.7619/\varepsilon_2 - 31.15/(\varepsilon_1\varepsilon_2) \tag{59}$$

(a)



(b)
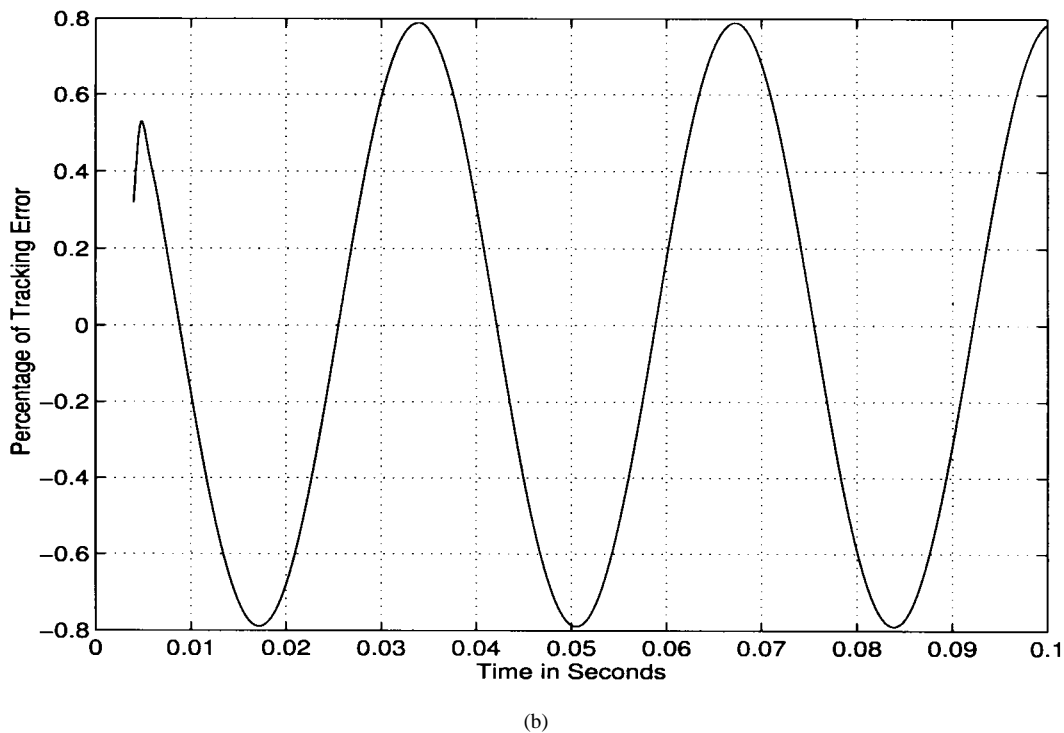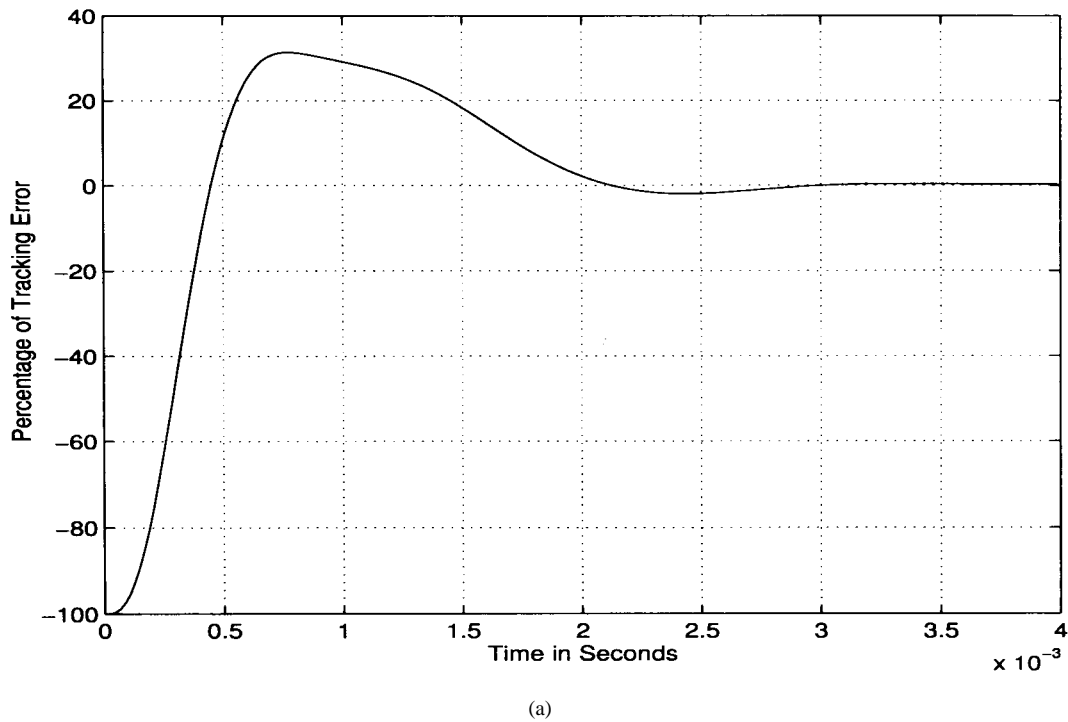
Fig. 10.   Tracking error for the 30-Hz cosine reference signal: (a) tracking error from 0 to 0.004 s and (b) tracking error from 0.004 to 0.1 s.

linear relationship between the tuning parameter $\varepsilon$ and the maximum frequency that a reference signal can have such that the corresponding tracking error is no larger than 1%, which is one of our main design specifications. The result is plotted inFig. 7.

Clearly, from Fig. 6, we know that due to the constraints on the control input, i.e., it must be kept within $\pm 112.5$ V, we have to select our controller with $\varepsilon_1 = \varepsilon_2 > 1/3370$.

From Fig. 7, we know that in order to meet the first design specification, i.e., the steady-state tracking errors should be less than 1% for reference inputs that have frequencies up to 30 Hz, we have to choose our controller with $\varepsilon_1 = \varepsilon_2 < 1/2680$. Hence, the final controller as given in (55)–(59) will meet all the design goals for our piezoelectric actuator system. i.e., (1) and (2), for all $\varepsilon_1 = \varepsilon_2 \in (1/3370, 1/2680)$. Let us choose $\varepsilon_1 = \varepsilon_2 = 1/3000$. We obtain the overall controller as in the
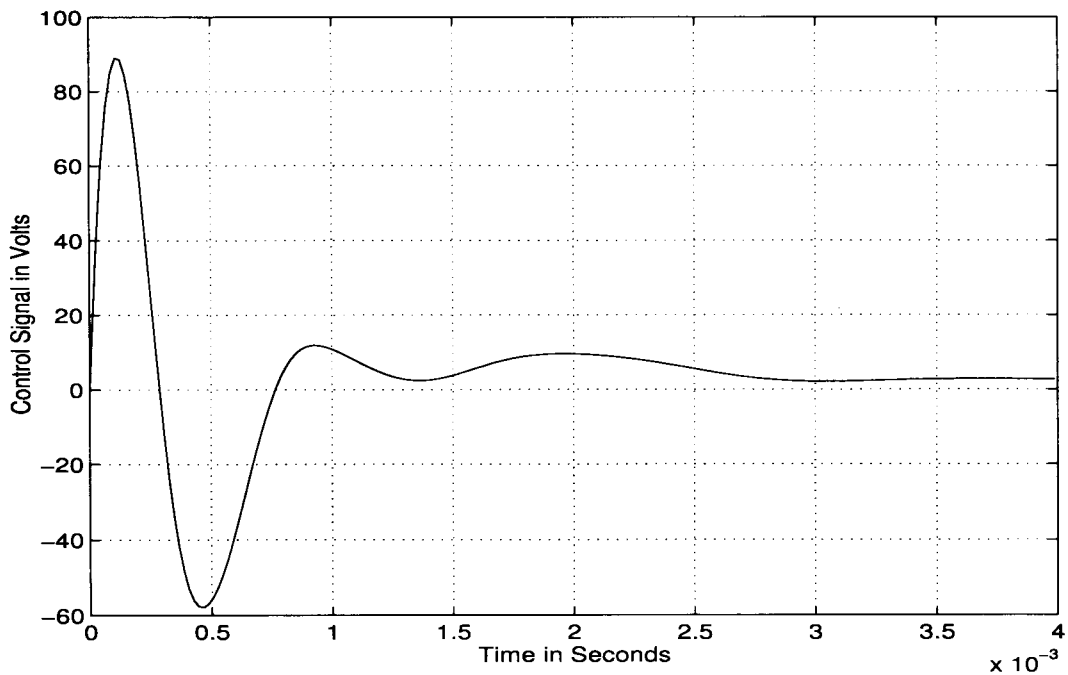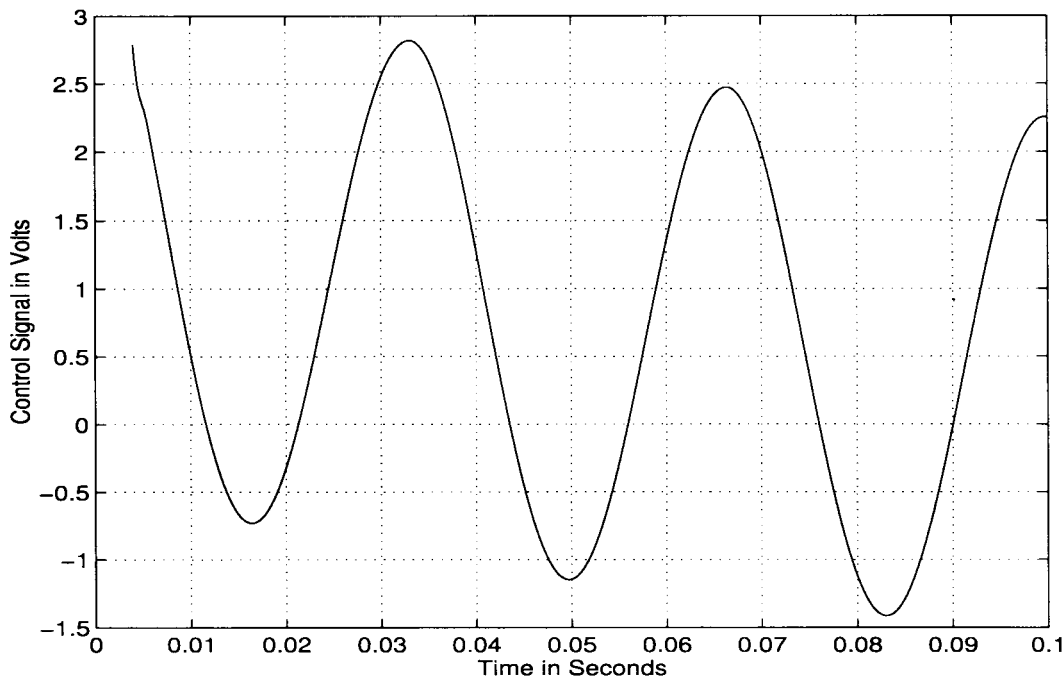
Fig. 11. Control signal for the 30-Hz cosine reference signal: (a) control signal from 0 to 0.004 s and (b) control signal from 0.004 to 0.1 s.

form of (55) with (60)–(63)

$$
A_{oc}
= \begin{bmatrix}
-14\,926.7085 & 0 & -2.16 \times 10^{11} & 3.24 \times 10^{14} \\
0.0315 & -1.6867 & 5.7118 \times 10^5 & 8.5677 \times 10^8 \\
0 & 0 & 0 & 0 \\
0 & 0 & 1 & 0
\end{bmatrix}
\tag{60}
$$

$$
B_{oc} = \begin{bmatrix}
-1.1569 \times 10^8 \\
281.9699 \\
1 \\
0
\end{bmatrix}, \quad
G_{oc} = \begin{bmatrix}
0 \\
0 \\
-1 \\
0
\end{bmatrix}
\tag{61}
$$

$$
C_{oc} =
\begin{bmatrix} -92\,879.9 & 2\,140\,967 & -1.6821 \times 10^{12} & -2.5232 \times 10^{15} \end{bmatrix}
\tag{62}
$$
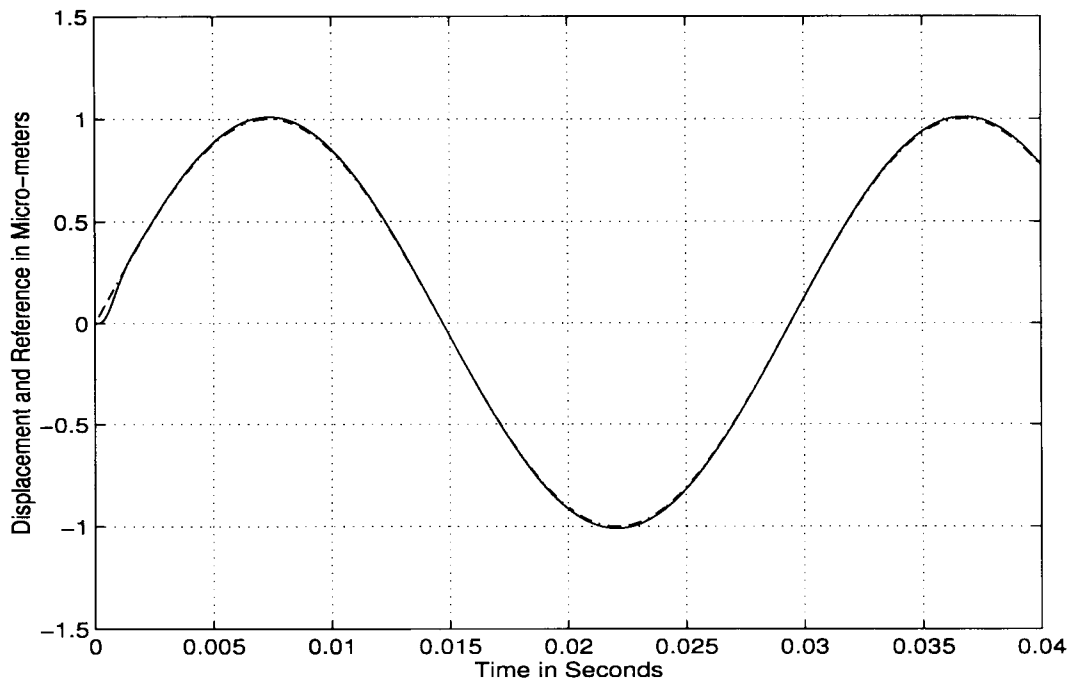
Fig. 12.   Responses of the displacement and the 34-Hz sine reference signal.
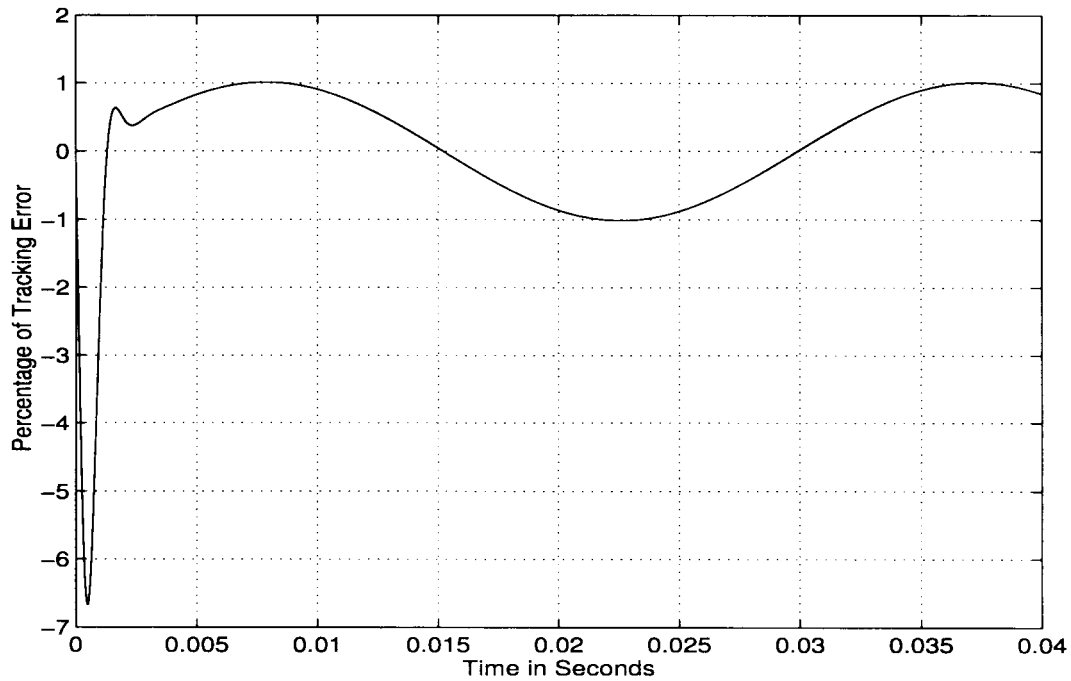


Fig. 13.   Tracking error for the 34-Hz sine reference signal.

and

$$D_{oc} = -8.304 \times 10^8. \tag{63}$$

The simulation results presented in the following are done using the MATLAB SIMULINK package, which is widely available everywhere these days. The SIMULINK simulation block diagram for the overall piezoelectric bimorph actuator system is given in Fig. 8. Two different reference inputs are simulated using the Runge–Kutta method in SIMULINK with a minimum step size of 10 ms and a maximum step size of 100 ms as well as a tolerance of $10^{-5}$. These references are: 1) a cosine signal with a frequency of 30 Hz and peak
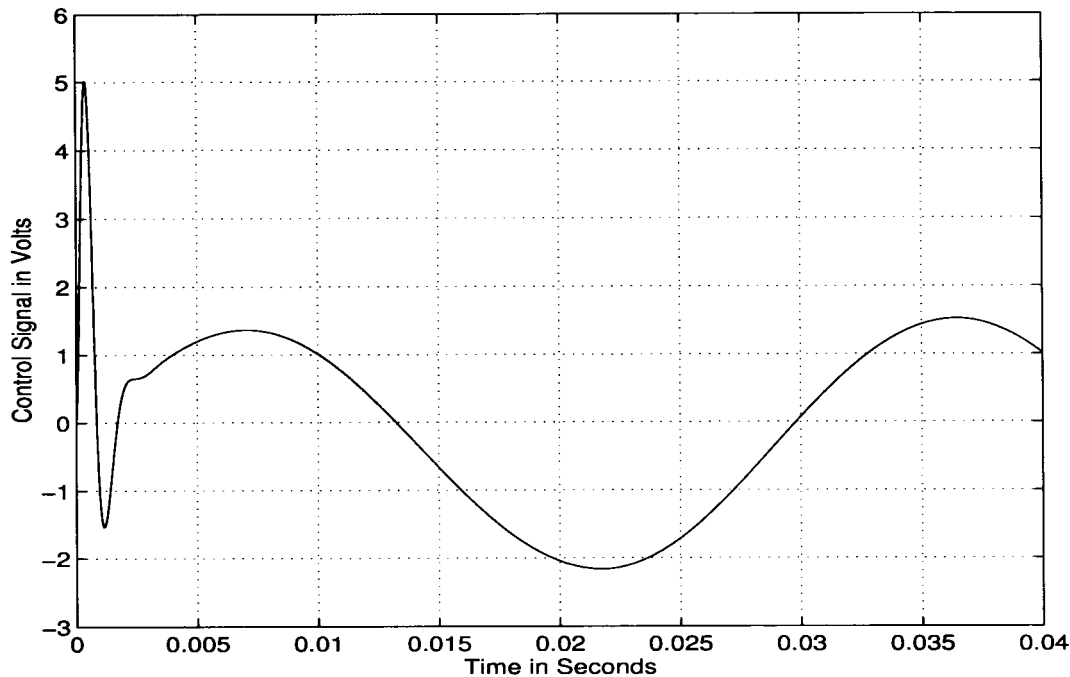
Fig. 14. Control signal for the 34-Hz sine reference signal.

magnitude of 1 $\mu$m, and 2) a sine signal with a frequency of 34 Hz and peak magnitude of 1 $\mu$m. The results for the cosine signal are given in Figs. 9–11. In Fig. 9, the solid-line curve is $x_1$ and the dash-dotted curve is the reference. The tracking error and the control signal corresponding to this reference are respectively given in Figs. 10 and 11. Similarly, Figs. 12–14 are the results corresponding to the sine signal. All these results show that our design goals are fully achieved. To be more specific, the tracking error for a 30-Hz cosine wave reference is about 0.8%, which is better than the specification, and the worst peak magnitude of the control signal is less than 90 V, which is of course less than the saturated level, i.e., 112.5 V. Furthermore, the 1% tracking error settling times for both cases are less than 0.003 s.

Finally, we note that because the piezoelectric actuator is designed to be operated in a small neighborhood of its equilibrium point, the stability properties of the overall closed-loop system of the nonlinear piezoelectric bimorph actuator should be similar to those of its linearized model. This fact can also be verified from simulations. In fact, the performance of the actual closed-loop system is even better than that of its linear counterpart.

## V. CONCLUDING REMARKS

We have designed an explicitly parameterized controller for a piezoelectric bimorph actuator, which has a nonlinear hysteresis. Our controller design was based on a so-called asymptotic time-scale and eigenstructure assignment technique of Chen *et al.* [6] and Ozcetin *et al.* [14]. The overall control system of our design turned out to be very successful and all design specifications were fully achieved. Currently, we are focusing on the implementation issues of our controller to the

real actuator system. We are planning to realize it using an AT&T DSP32C (50 MHz). Of course, they are many things needed to be taken care of in a real implementation. These would be our future tasks.

## REFERENCES

[1] R. C. Booton, Jr., "Nonlinear control systems with random inputs," *IRE Transactions on Circuit Theory,* vol. CT-1, pp. 9–18, 1954.
[2] T. P. Chang, "Seismic response analysis of nonlinear structures using the stochastic equivalent linearization technique," Ph.D. dissertation, Columbia University, 1985.
[3] B. M. Chen, "Theory of loop transfer recovery for multivariable linear systems," Ph.D. dissertation, Washington State University, 1991.
[4] ——, "Linear systems and control toolbox," Department of Electrical Engineering, National University of Singapore, unpublished, 1994.
[5] B. M. Chen, A. Saberi, and U. Ly, "A noniterative method for computing the infimum in $H_\infty$-optimization," *Int. J. Contr.,* vol. 56, pp. 1399–1418, 1992.
[6] ——, "Closed-loop transfer recovery with observer-based controllers, Part 1: Analysis and Part 2: Design," *Control and Dynamic Systems: Advanced in Theory and Applications,* vol. 51, pp. 247–348, 1992.
[7] T. K. Caughey, "Derivation and application of the Fokker-Planck equation to discrete nonlinear dynamic systems subjected to white random excitation," *J. Acoust. Soc. Amer.,* vol. 35, no. 11, pp. 1683–1692, 1963.
[8] S. T. Crandall, "Perturbation techniques for random vibration of nonlinear systems," *J. Acoust. Soc. Amer.,* vol. 35, no. 11, pp. 1700–1705, 1963.
[9] L. S. Fan, H. H. Ottesen, T. C. Reiley, and R. W. Wood, "Magnetic recording head positioning at very high track densities using a microactuator-based, two stage servo system," *IEEE Trans. Ind. Electron.,* pp. 222–233, 1995.
[10] Z. L. Lin, A. Saberi, and B. M. Chen, "Linear systems toolbox," Washington State University, Tech. Rep. no. EE/CS 0097, 1991.
[11] T. S. Low and W. Guo, "Modeling of a three-layer piezoelectric bimorph beam with hysteresis," *J. Microelectromech. Syst.,* vol. 4, pp. 230–237, 1995.
[12] R. H. Lyon, "Response of a nonlinear string to random excitation," *J. Acoust. Soc. Amer.,* vol. 32, no. 8, pp. 953–960, 1960.
[13] D. K. Miu and Y. C. Tai, "Silicon micromachined SCALED technology," *IEEE Trans. Ind. Electron.,* pp. 234–239, 1995.

[14] H. K. Ozcetin, A. Saberi, and P. Sannuti, "$H_\infty$ almost disturbance decoupling for nonstrictly proper systems—A singular perturbation approach," *Contr. Theory Advanced Technol.,* vol. 9, pp. 203–245, 1993.

[15] A. Saberi and P. Sannuti, "Time-scale structure assignment in linear multivariable systems using high-gain feedback," *Int. J. Contr.,* vol. 49, pp. 2191–2213, 1989.

[16] P. Sannuti and A. Saberi, "A special coordinate basis of multivariable linear systems—Finite and infinite zero structure, squaring down and decoupling," *Int. J. Contr.,* vol. 45, no. 5, pp. 1655–1704, 1987.

[17] A. A. Stoorvogel, *The $H_\infty$ Control Problem: A State-Space Approach.* Englewood Cliffs: Prentice-Hall, 1992.

[18] K. M. Tsuchiura, H. H. Tsukuba, H. O. Toride, and T. Takahashi, "Disk system with subactuators for fine head displacement," US Patent no. 5189578, 1993.

[19] S. Weiland and J. C. Willems, "Almost disturbance decoupling with internal stability," *IEEE Trans. Automat. Contr.,* vol. 34, pp. 277–286, 1989.

[20] K. Zhou and P. Khargonekar, "An algebraic Riccati equation approach to $H_\infty$ optimization," *Syst. Contr. Lett.,* vol. 11, no. 1, pp. 85–91, 1988.

**Chang-Chieh Hang** (S'70–M'73–SM'90–F'98) received the bachelor's degree with First Class Honors in electrical engineering from the University of Singapore in 1970. He received the Ph.D. degree in control engineering from the University of Warwick, U.K., in 1973.

From 1974 to 1977, he worked as a Computer and Systems Technologist in the Shell Eastern Petroleum Company (Singapore) and the Shell International Petroleum Company (The Netherlands). He was a Visiting Scientist in Yale University in 1983, and in Lund University in 1987 and 1992. Since 1977, he has been with the National University of Singapore, serving in various positions including being the Vice-Dean of the Faculty of Engineering and Head of the Department of Electrical Engineering. Since October 1994, he has been Deputy Vice-Chancellor. His major area of research is adaptive control in which he has published one book and 170 international journal and conference papers. He holds four patents.

Since March 1992, Dr. Hang has been Principal Editor (Adaptive Control) of the *Automatica* Journal.

**Ben M. Chen** (S'89–M'92) was born in Fuqing, Fujian, China, on November 25, 1963. He received the B.S. degree in mathematics and computer science from Amoy University, Xiamen, China, in 1983, the M.S.E.E. degree from Gonzaga University, Spokane, WA, in 1988, and the Ph.D. degree in electrical and computer engineering from Washington State University, Pullman, in 1991.

He was a Software Engineer from 1983 to 1986 in the South-China Computer Corporation, and was an Assistant Professor from 1992 to 1993 in the Electrical Engineering Department, State University of New York at Stony Brook. Since August 1993, he has been with the Department of Electrical Engineering, National University of Singapore, where he is currently a Senior Lecturer. His current research interests are in robust control, linear system theory and control applications. He is the author of the monograph, $H_{[\infty]}$ *Control and Its Applications* (New York: Springer-Verlag, 1998), and coauthor of the books, *Loop Transfer Recovery: Analysis and Design* (New York: Springer-Verlag, 1993), $H_2$ *Optimal Control* (Englewood Cliffs, NJ: Prentice-Hall, 1995), and *Basic Circuit Analysis* (Singapore: Prentice-Hall, 1996–1998).

Dr. Chen currently serves as an Associate Editor on the Conference Editorial Board of the IEEE Control Systems Society and an Associate Editor of IEEE TRANSACTIONS ON AUTOMATIC CONTROL.

**Yi Guo** was born in Fuzhou, Fujian, China, on December 31, 1968. He received the B.S. degree in electrical engineering from Zhejiang University, Hangzhou, China, in 1990, the Master of Engineering Degree in electrical engineering from National University of Singapore, in 1996.

He was a Senior Hardware Engineer from 1990 to 1994 in the New Century Data Equipment Corp., China. Since April 1996, he has been with the Asian Design Center of the Hewlett Packard Singapore, where he is currently an Engineer.

**Tong H. Lee** (M'88) received the B.A. degree with First Class Honors in the Engineering Tripos from Cambridge University, U.K., in 1980, and the Ph.D. degree from Yale University, New Haven, CT, in 1987.

Currently, he is an Associate Professor and Head of the Control Division at the Department of Electrical Engineering of the National University of Singapore. His research interests include adaptive systems, knowledge-based control, and mechatronics.

Dr. Lee was a recipient of the Cambridge University Charles Baker Prize in Engineering.

**Siri Weerasooriya** received the B.Sc. degree from University of Moratuwa, Sri Lanka, in 1986. He received the M.S.E.E. and Ph.D. degrees from the University of Washington, Seattle, in 1989 and 1992, respectively. He joined the Data Storage Institute in Singapore as a founder member of technical staff and headed its Servo Division until 1997. He currently works for Quantum Corporation as a Servo Design Engineer. His expertise is the application of precision motion control techniques in rotating memory devices and related subsystems.